Structural monitoring of a highway bridge using passive noise recordings from street traffic

Johannes Salvermoser, Céline Hadziioannou, Simon C. Stähler
Department for Earth- and Environmental Sciences
Ludwig-Maximilians-University
Theresienstrasse 41, 80333 Munich

(Dated: March 3, 2015)

Structural damage on bridges presents a hazard to public safety and can lead to fatalities. This article contributes to the development of an alternative monitoring system for civil structures, based on passive measurements. Cross-correlations of traffic noise recorded at geophone receiver pairs were found to be sufficiently stable for comparison and sensitive to velocity changes in the medium. As such velocity variations could be caused by damage, their detection would be valuable in structural health monitoring systems. We exploited the Passive Image Interferometry (PII), a method introduced for seismological applications, to quantify small velocity fluctuations in the medium and thereby observe structural changes. Evaluation of more than two months of geophone recordings at a reinforced concrete bridge yielded velocity variations $\frac{\Delta v}{v}$ in the range of -1.5% to +2.1%. We were able to correlate our observations with temperature measurements, and found great resemblance between these two completely uncorrelated data sets. Using a linear regression approach, we could identify the relationship between temperature and velocity variations of on average $0.064\%^{\circ}\mathrm{C}^{-1}$. This value corresponds well with other studies on concrete structures.

PACS numbers: 43.40.Le, 43.40.Ph, 43.20.Jr, 43.20.Fn

I. INTRODUCTION

Large-scale structures, especially heavily used ones like bridges, operate over decades until eventually their capacity and reliability expires. For cost minimization reasons, most operators try to run the structures as long as possible. Since a failure would result in high damage to lives and property, this is only possible with a reliable monitoring system in place. The most common technique for monitoring is regular visual inspection of the structure combined with localized non-destructive measurements. Since this kind of inspection is expensive and personnel-intensive, their rate is very limited, mostly to once a year or less. Moreover, they concentrate on typical points of failure, such as the casing of tendons and places where run-off water from the street can cause chemical degradation of the concrete via the alkali-silica reactions. Therefore, global monitoring techniques, where a small set of measurements allows to check the overall state of a structure at once, are extremely promising.

One candidate is modal measurements, which aim to detect perturbations of modal parameters (natural frequencies, modal shapes) caused by structural changes. These have first been used in combination with active vibration sources, often in big monitoring campaigns on bridges and dams. Due to the enormous logistical effort and poor temporal resolution of active (input-output) measurements with large vibration sources, recently techniques employing ambient vibrations (output-only) have been developed[1]. New, more sensitive transducers and A/D converters made it possible to extract information from smaller, traffic- and wind-induced vibrations.

Increasing computational power allows to simulate damage scenarios on more and more complex structures. Using finite element (FE) models and damage detection algorithms improves "automated" SHM (e.g.[2,3,4]). Unfortunately, the underlying FE models are usually only an incomplete representation of the structure and environmental effects, especially temperature variations, are hard to gauge. This affects the overall reliability of automated SHM methods.

Time-domain based approaches like the ultrasonic pulse velocity method (reviewed in[5]) have many applications in small-scale testing. Laboratory experiments on concrete samples[6,7,8] showed that weak changes in material properties (caused by stress or temperature variations) can be detected by measuring the direct wave (pulse), emitted by a kHz-source, at a nearby receiver. However, reducing environmental effects is still complex, the wave range is limited to a few meters and many measurement campaigns would be needed to achieve a sufficiently high tem-

poral resolution for monitoring.
The idea of monitoring small changes in material properties with passive methods was adapted from seismology.[9] showed that the Green's function between two receivers can be retrieved from diffuse wavefields (eg. ambient noise) recorded at the receivers. For uniformily distributed noise sources and long records, the cross-correlation between the noise records converges towards the Green's function, which contains all the information about the medium in between. Among others,[10] showed that this principle also applies for seismic noise if cross-correlations are averaged over sufficiently long periods (weeks to months). In terms of using the noise correlation method to monitor changes in seismic velocity,[11] elaborated on the method and called it Passive Image Interferometry (PII). This method, which is further explained in sec. II, was subsequently used to monitor fault zones (eg.[12]) and active volcanoes (eg.[13]).

This study aims toward the development of a time-domain technique for monitoring of civil structures. It applies the seismological method of passive image interferometry to small scales. To that end, 27 geophones were installed in the girder of a 229 m long highway bridge, and continuously recorded vertical motion of the bottom slab (sec. III). The main observation is that the recorded signal is dominated by traffic induced noise and that the strongest peaks come from cars crossing the extension gap at either end of the bridge (sec. III.B). Section IV explains how that signal can be used for passive image interferometry. The results, presented in sec. V show that effect of temperature variations on the elastic wave velocities can be measured well with PII using traffic noise. This is promising, as it means the method of PII could be applied to a range of structures where strong cultural noise sources, like car traffic, are available. Our results are tested for biases caused by temperature sensitivity of the sensors in sec. VI.A and compared with prior studies using active measurements on bridges and in the laboratory in sec. VI.B. The discussion concludes with an examination of the relation between temperature and velocity changes (sec. VI.C).

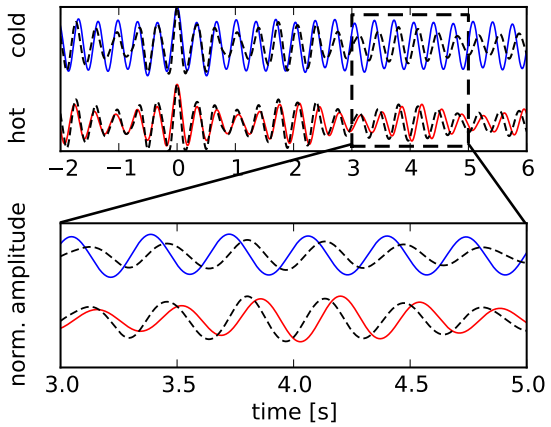

FIG. 1. Real data example for extreme temperature cases; blue (top): cross-correlation of 1 hour of noise recorded at two receivers at temperature of -23°C, red (bottom): same for temperature of +13°C, black dashed line: reference signal consisting of average of all cross-correlations from the total recording time. The signal recorded on a cold day is clearly compressed compared to the reference, the signal corresponding to a hot day is stretched.

II. METHOD

A. Coda-wave Interferometry

The coda wave interferometry method was described by[14], and it allows to extract changes in wave propagation speed. Measuring velocity changes by using the travel time differences of direct wave arrivals has a limited resolution. However, for a given homogeneous wave speed change, the traveltime delay dt will increase linearly with lapse time[15]. Coda wave interferometry takes advantage of this fact by measuring the shifting of a whole wave-train at the late part of a seismic signal, also named the *coda*. By doing so, it enables an exact measurement of small relative travel time changes, as the absolute changes accumulated in the seismic coda are larger. Moreover, due to contributions from many phases, the coda is particularly sensitive to small variations in material properties like scatterer distribution. A relative velocity change $\frac{\Delta v}{v}$ is related to a relative runtime change $\frac{\Delta t}{t}$ in the medium. Assuming a mostly homogeneous velocity change $\frac{\Delta v}{v} = \epsilon$ in the medium, we expect to observe a perturbed time series $h'(t)$:

$$h'(t) = h(t(1-\epsilon)) \tag{1}$$

This effect can be quantified by means of the stretching method[11,16]:
From equation 2, we obtain a correlation coefficient CC that represents a measure of similarity for a certain window $t \pm \frac{T}{2}$ and a stretching factor ϵ. The

signal $h'(t)$ is stretched by different values of ϵ to fit it to the reference trace $h(t)$. The best fitting velocity change (grid search optimization) is found at the ϵ for which CC reaches a maximum.

$$CC(\epsilon) = \frac{\int_{t-T/2}^{t+T/2} h'[t(1-\epsilon)]\, h[t]\, dt}{\sqrt{\int_{t-T/2}^{t+T/2} h'^2[t(1-\epsilon)]\, dt \cdot \int_{t-T/2}^{t+T/2} h'^2[t] dt}}, \tag{2}$$

where $h(t)$ is the reference function (RCF), $h'(t)$ the variable function (CCF), ϵ the stretching factor ($= \frac{\Delta v}{v}$), t the lapse-time and $T/2$ the lapse-time window.

B. Noise cross-correlation

In order to obtain repeatable signals, we will use the noise correlation method. According to[10,17], the correlation of uniformly distributed noise, recorded at two receivers over a sufficiently long period, converges toward the Green's function between those receivers. Since the Green's function contains all information about elastic parameters, comparing the Green's functions calculated at different times allows to detect and characterize changes in these parameters[11]. Changes in the elastic parameters could be caused by varying internal stress states, temperatures, or structural damage.
The method should work even for short noise durations. While the cross-correlated function (CCF) might not have converged against the Green's function, it can still be used to detect temporal changes[18]. If the correlations are sufficiently stable, complete convergence is not necessary to monitor velocity variations. In our case hourly CCFs were found to be sufficiently stable for comparison and sensitive to velocity changes in the medium.

We want to measure velocity changes caused by the temperature variations in a reinforced concrete bridge. Temperature variations most likely have a homogeneous effect on seismic velocity in our measurements. In this case, the shape of the coda is preserved due to a stable scatterer distribution and therefore the linear relation $\frac{dv}{v} = -\frac{dt}{t}$ applies.

III. MEASUREMENT SETUP

A. Setup

To record traffic noise, 27 standard geophones (f_{corner} = 4.5 Hz, R = 380 Ω) were installed. To protect the instruments against weather, they were installed at the bottom slab of the accessible box girder below the deck slab (see fig. 2b). To ensure constant coupling, they were fixed by cementing them to the concrete (fig. 2d). From the eastern end of the bridge, the array with a spacing of 4 m extends 100 m toward the center of the 229 m long bridge (fig. 2a).
The bridge supports a road with two traffic lanes, one for each direction. It is not fixed at the ends to allow for variations of the length caused by thermal expansion. Thus, expansion joints can be found at both ends of the bridge. Since the Steinachtal bridge is a rather recent construction (*2008), we do not expect damage to interfere with our measurement. Noise generation on this bridge is supposed to be primarily driven by traffic. Vehicles passing the expansion joints produce blasts that excite different waves with a broad spectrum. Compressional waves have the highest velocities and frequencies. However, since their wavelength is large compared to the width of the deck slab, only very high frequencies ($\gg$ 10 kHz) can propagate freely. At these frequencies, which are outside the range of our instrument sensitivity, attenuation becomes dominant. Therefore, we concentrated on longer period flexural waves of the whole superstructure. These propagate back and forth between the ends of the bridge after excitation. We can correlate the recordings between each pair of receivers on the bridge, as the direct and flexural waves always pass both.
In two measurement periods (2011/12/21–2012/01/14 and 2012/02/01–2012/03/10), traffic noise was recorded by the geophone array at a

Bridge data	
length	229 m
dist. betw. supports	42.5-48-48-48-42.5 m
width of deck	12.00 m
width of base plate	5.00 m
thickness of deck	0.25 m
traffic volume	10-200 vehicles/hour

TABLE I. Characteristics of the bridge

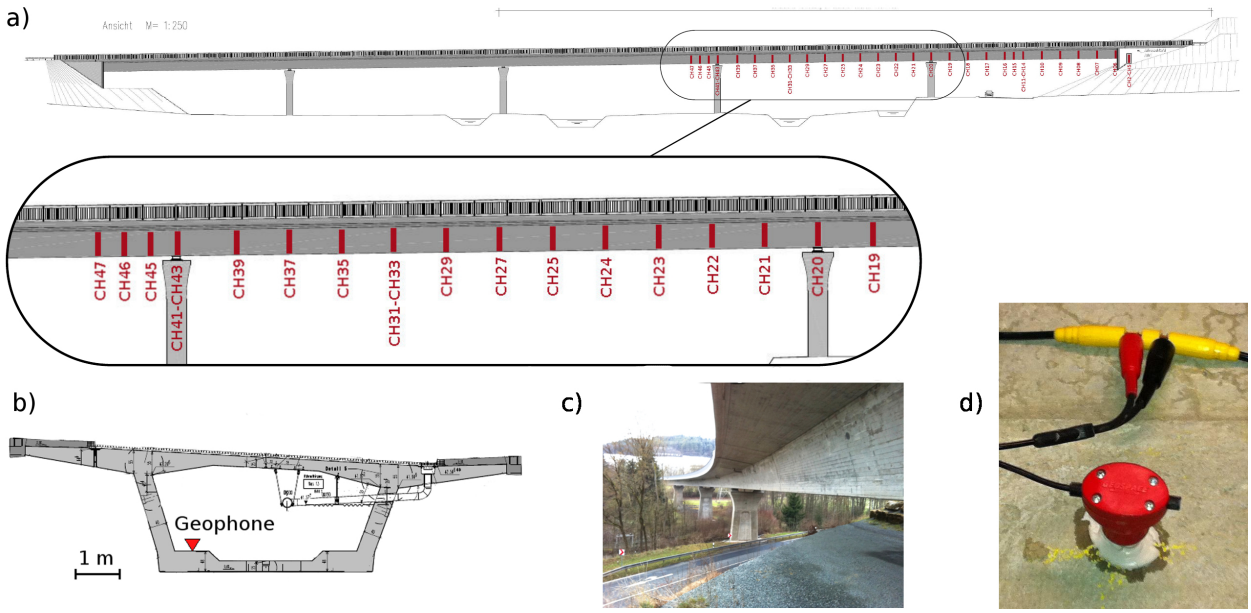

FIG. 2. (a) Lateral view on the Steinachtal bridge (scheme). Bars indicate the positions of geophones in the box girder. (b) Cross-section of the box girder with geophone position indicated by a triangle. (c) The photo shows the bridge in construction state, viewed from below. (d) Fixing of a geophone to the bridge. The instrument was screwed on a footplate, which was then cemented on bridge. It was not possible to drill holes into the bridge itself.

sampling frequency of 500 Hz. The traces of all geophone-channels were continuously stored in SEG2-format streams of 32 s length.
Two sets of temperature data were available for evaluation of the temperature effect on the Steinachtal bridge. One detailed set was available for 2012, i.e. for the first 10 days of measurement. It contains two temperature time series at the surface of the road and at 30 cm depth inside the concrete deck slab. A second set of temperature measurements from the meteorological station Kronach about 10 km away was received via DWD (Deutscher Wetterdienst). We obtained air-temperature data with an hourly resolution that was measured 5 cm above the ground, which came closest to the conditions on the bridge. Apart from slightly lower fluctuation amplitudes in the in-bridge data, the agreement between the measurements of the two sites was surprisingly good.

B. Signals

Typically, the traffic-noise recordings feature rather flat background noise and a number of distinct peaks depending on traffic activity. As mentioned before, these peaks are produced by vehicles passing the bridge. Their occurrence rate depends on the traffic volume which is especially high during rush hours and low between midnight and 4 a.m..
A priori, it was unproved whether there is a constraint on usability in terms of correlation. Hence, in the following we conducted an automated separation between "calm" and "noisy" traces to evaluate them separately. In this context "calm" means no vehicle passed the bridge in the 32 s time window and "noisy" means that vehicles produced blasts leading to distinct peaks in the seismograms. Eventually, using the noisy traces turned out to be necessary because of the poor temporal coverage by the calm traces.

A closer look at the single events reveals that they are not simply uniform peaks but clearly display notable features (fig. 3). Aside from the fact that one event lasts for 20-30 s, there is a clear onset and a fading out over several seconds at the end. Two distinct peaks can be found in the spectrogram of fig. 3. They are related to high amplitude direct waves produced by the vehicle passing the expansion gaps on either ends of the bridge. We can also observe slowly decaying amplitudes following the second hit which analogously appears in the spectro-

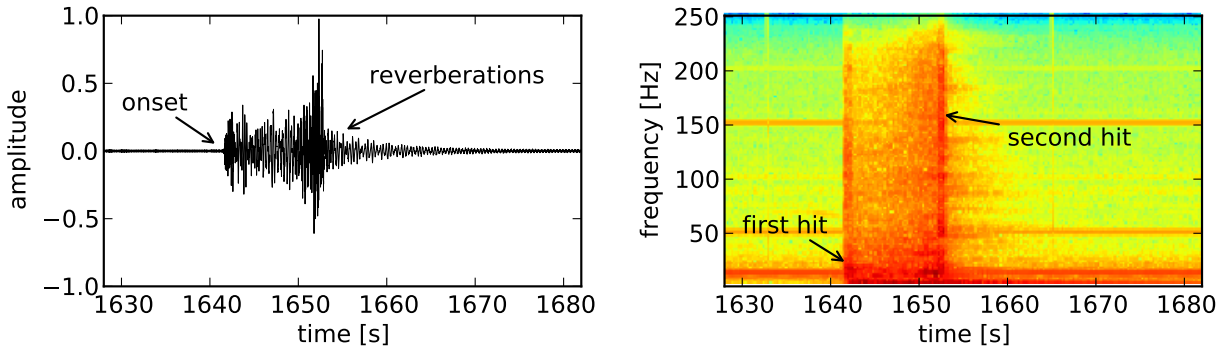

FIG. 3. (a) Waveform recorded for a car passing the bridge and (b) spectrogram for this event. Characteristic features of this signal are the clear onsets (corresponding to the vehicle passing the expansion gap at either end of the bridge) and distinct reverberations. The amplitudes suggest that the car passed the more distant extension gap first, i.e. that it was traveling east-ward (compare fig. 2a). The time difference of roughly 10 seconds between the crossings of the two gaps correspond to a car velocity of roughly 80 kph, which is indeed the allowed velocity.

gram, but such that high frequency amplitudes decay much faster than lower ones. Low frequencies are associated with flexural waves (reverberations) propagating back and forth between the unbound ends of the bridge.

In fig. 3b, the horizontal, permanently excited frequency bands at 12.5 Hz, 50 Hz, 100 Hz and 150 Hz are most likely related to electro-magnetic (e-m) noise induced by the electric lines which are required for power supply (light, measurements).

The unfiltered spectrum (fig. 4) shows five higher peaks between 2 Hz and 6 Hz, likely associated with natural frequencies of the bridge.

We concentrated on the frequency band containing the bridge's natural frequencies and the long lasting, low-frequency reverberations, i.e. 2–8 Hz.

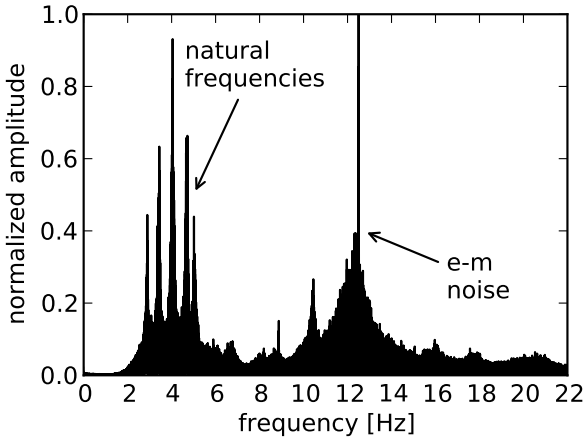

FIG. 4. Normalized spectrum for 6 hours of traffic noise recorded at a single geophone. The measurement was not corrected for instrument response, which explains the drop below 2 s period. The peak at 12.5 Hz is constant over the whole measurement period, while the peaks between 2 and 5 Hz vary slowly over time (see fig. 7).

IV. PROCESSING

Here we will use noise cross-correlation as explained in section II.B. In our experiment, the conditions for a diffuse wavefield are not fulfilled, as the seismic waves are excited only at the two ends of the examined bridge and propagate along one axis. Due to this unilateral source distribution, it was not possible to reconstruct Green's functions between receivers. Consequently, the aim was to prepare appropriate CCFs that capture the environmental conditions of the bridge regardless. With these we sought to uncover small changes in seismic velocity.

Most of the processing was done with toolboxes of ObsPy[19] and NumPy[20,21].

A. Filtering and cross-correlation

After de-trending, the data was pre-filtered to a 0.2–24 Hz band with a bandstop to avoid the 12.5 Hz e-m noise using Butterworth zero-phase filters. The

high-pass was set to minimize the impact of low frequency instrumental drift.
As a tool to remove non-stationary events in seismic records, the one-bit normalization (reviewed by **(author?)** [22]) is suitable to diminish the impact of direct surface waves on cross-correlations by decreasing their distinctive amplitudes (compared to reverberations). The one-bit cross-correlation C^{ob}_{AB} is defined as:

$$C^{ob}_{AB}(t) = \int sgn[A(\tau)] \cdot sgn[B(t+\tau)]d\tau \qquad (3)$$

where $A_p(\tau)$ and $B_p(\tau+t)$ denote the signals from a point source P recorded at the receivers A, B. This operation is non-linear, but as it preserves the phase it does not interfere with our results.
Our correlation functions were produced by first merging the 32 s records to 2-minute signals, calculating the CCFs and stacking about thirty of these to hourly stacks. Several receiver pairs with different inter-receiver distances (4–90 m) and locations on different sections of the bridge were tested in this context.
In order to evaluate the stability of the resulting CCFs, we calculated the signal-to-noise ratio (SNR) as follows (eq. 4).

$$\text{SNR} = \frac{max(\mid h(t) \mid)}{std(h(t))}, \qquad (4)$$

where $h(t)$ is the cross-correlation function. As more 2-minute CCFs are stacked, the SNR increases. From this analysis, we concluded that 1 hour long CCFs (SNR $\geq$ 4000) are stable and reproducible enough for further use.
Several methods have been proposed to evaluate velocity changes in media. In the case of passive image interferometry (PII)[11], the stretching method has proven to be adequate. As described in eq. 2, our hourly CCFs are compared to a reference correlation function (RCF). In our case the RCF is represented by a normalized stack of all hourly CCFs for the particular frequency band and receiver pair (e.g. RCF for: 2–8 Hz and CH27–CH37).

B. Effect of temperature changes

Our main focus was the observation and evaluation of temperature induced velocity changes. The general assumption in that context is that the wave velocity decreases with increasing temperature in the medium, thus the travel time of the waves increases. This is presumably caused by an alteration of the elastic moduli (Young's Modulus, etc.) that also affect the propagation of seismic waves. All elastic parameters must be considered to be temperature dependent. Additionally, thermal expansion will affect our measurements. This effect is separately discussed in section VI.
Figure 1 illustrates differences in CCF waveform shapes (resp. travel-times) for two extreme cases of high and low temperature regime extracted from our measurements. When compared to the reference function, either the CCF is compressed (cold) or stretched (hot). This figure also clarifies why we examine the coda of the CCF and do not investigate the first arrivals: the effect increases the longer the wave is traveling in the medium (longer wave paths) and thus the later in the CCF.
The time window we use for our analysis extends from 0.05 s to 11.5 s in the causal part (positive lapse times) of the CCF. The part before 0.05 s is skipped to avoid the direct arrivals at all receivers and the 11.5 s limit corresponds to a minimum 75%-decay time for the CCFs, after which the waveforms become less deterministic.

V. RESULTS

The evaluation of velocity changes caused by temperature fluctuations on the bridge yielded interesting results.
As described in section II, we used the stretching method to measure relative wave speed changes dv/v. Most of the associated correlation coefficients were larger than 90%, decreasing slightly during low-traffic periods at night and rising to peaks of 99% at the daily rush hours.
We discovered a striking resemblance between the resulting curve of velocity variations over time and the time series of temperature measurements for the same period. In fig. 5 and fig. 6 instead of $\frac{\Delta v}{v}$ we display $\frac{\Delta t}{t} = -\frac{\Delta v}{v}$ to more easily compare the shape with that of the temperature values. For increasing temperatures, we observe increasing traveltime delays but decreasing velocities.
When considering the trends of both curves in the figures, one recognizes a constant time shift between the two measurements that can be explained by thermal diffusion. Since we measure air temperature for this period, there is a natural delay time in which the ambient temperature propagates into the concrete of the bridge where it then induces velocity variations. In this context, time lags in the order of 3 hours

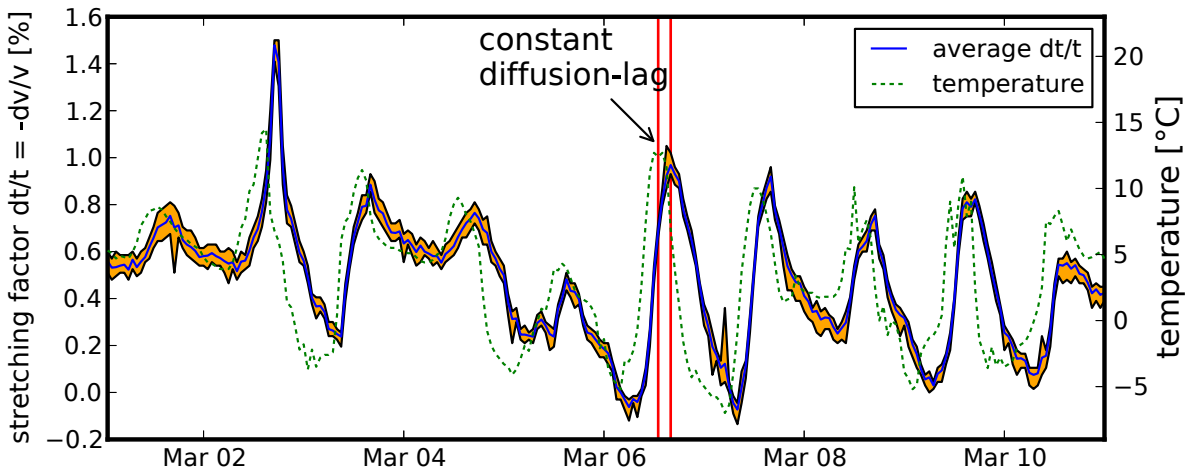

FIG. 5. Velocity variations at receivers 35/22 for the first days of March 2012. Relative velocity variations averaged over 8 receiver pairs are compared to temperature measurements. The shaded area indicates the standard deviation of the velocity variation curve, while the vertical lines show the constant thermal diffusion lag of about 3 hours.

were observed. This will be reconsidered in the discussion. Apart from the time shift, the agreement between these two completely independent measurements is very high. Furthermore, the eight different receiver pairs we tested show very similar results, as can be seen from the small variance around the average velocity variation curve in fig. 5.

Considering the results of different parts of the measurement period, we discovered clear differences in their patterns. For December 2011 and January 2012 the velocity variations are not dominated by daily cycles but by a rather flat long-term evolution. In contrast, February and March 2012 show distinct daily fluctuations associated in both temperature and velocity variations.
Figure 6 reveals that this is a meteorological issue. The difference in variation pattern seems to be related to cloud cover or rather daily hours of sunlight, which are plotted in this figure for comparison. Temperature fluctuations tend to be higher on days of low cloudiness as clouds screen the ground from direct insulation by day, simultaneously acting as an insulating layer between ground and cold, upper troposphere during night.

Further investigations were performed with regard to other environmental effects and their influence on relative velocity variations. Environmental data was recorded by instrumentation installed permanently on the bridge for different road condition monitoring purposes. We found that neither humidity of the road, nor precipitation itself, nor wind speed (peak or average), feature any correlation with the observed patterns.

For the overall measurement period we obtained relative velocity variations in the range of -1.5% to +2.1%, while air temperature data yielded values between +14°C and -23°C.
To numerically quantify the relationship between temperature and velocity change and make our results comparable to prior studies, we estimated relative velocity variation rates (VVR) with a simple linear regression approach. We fitted intervals of a few days of temperature-velocity-variation-pairs with a linear regression. From its slope, we inferred the relative velocity variation per °C. The quality of this rate was then verified by removing the inferred temperature effect from the original velocity variation curve. To do this, the temperature curve was scaled using the calculated variation rate (VVR), and subtracted from the velocity changes. Assuming no damage occurred during the measurement period, this should result in a flat response.

For short intervals, up to 48 hours, this method worked reasonably well, yet for longer intervals the subtraction did not result in a flat response. One of the reasons for this is that the effect of temperature on velocity in the bridge is found to be non-linear. Potential explanations for this behavior will be reasoned in the discussion. Consequently, the VVR determined for one period is not applicable for others, particularly if there was a significant difference in temperature range.

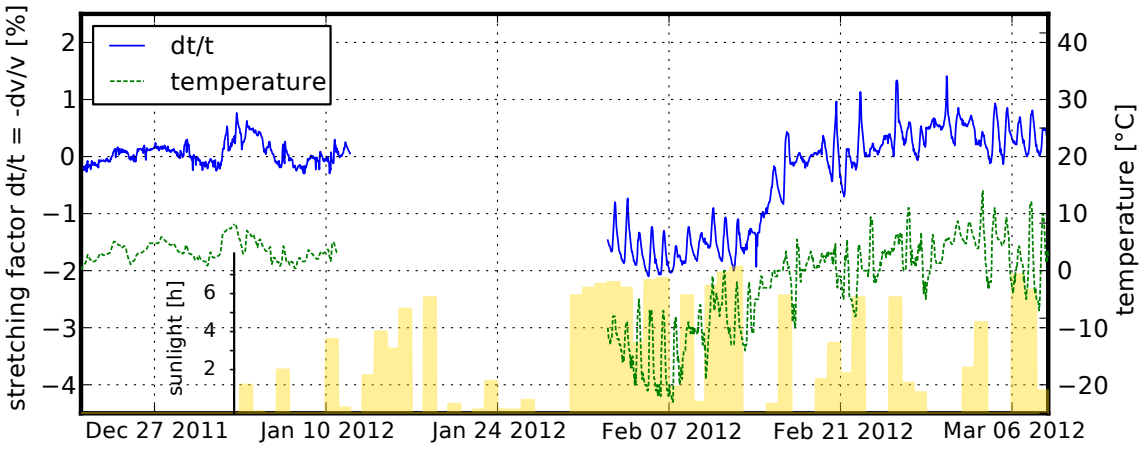

FIG. 6. Velocity variations at receivers 35/22 for the complete measurement period. Hours of daily sunlight (histogram) and temperature (dotted line) are plotted to emphasize their importance as environmental factors influencing the seismic velocity on the Steinachtal bridge. It can be seen that sunny days have higher amplitudes in the diurnal velocity variations. This may be explained by stronger temperature gradients in the concrete due to surface heating by direct solar irradiation.

VI. DISCUSSION

In an experiment covering more than two months of recording on the Steinachtal bridge, long-term trends and daily variations of temperature could be clearly traced by means of velocity variations.

A. Reliability tests

The results presented in the previous section were tested for plausibility regarding different physical effects that could affect the outcome.

First of all, the impact of thermal expansion was considered: a lower density for higher temperatures is equivalent to an increase in volume. In other words, as temperatures fluctuate the bridge experiences thermal expansion. However,[23] states that the effect is small, of the order of 6-14 $\cdot 10^{-6}$. Therefore, associated variations in length are orders of magnitude too small to explain the observed wave speed fluctuations.

The impulse response of the geophones could be affected by temperature variations as well. The corner frequency of the devices can shift as re result of a temperature change, which can generate significant phase shifts. This would produce delays in the seismogram that could be misinterpreted as velocity variations in the medium. In order to assess whether

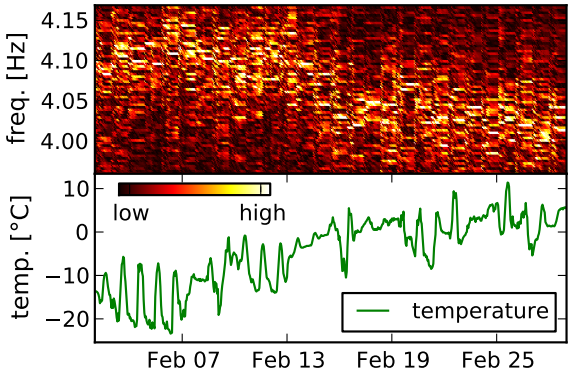

FIG. 7. Eigenfrequency evolution for a natural frequency around 4 Hz. Each vertical column in the top figure consists of an hourly spectrum. The color bar qualitatively indicates the corresponding amplitudes. Bottom: Temperature measurement for the same period. The Eigenfrequency follows the temperature curve, but with a much lower temporal resolution and higher noise level than the velocity measurements presented in fig. 6.

a change in instrument response could indeed be responsible for our observed changes in wave speed, we perform a synthetic test. We use a signal recorded by one of the geophones, and deconvolve the instrument response. Then, the signal is convolved with

another, artificial response. This artificial response is modified in such a way that the corner frequency is shifted, to simulate a temperature induced shift and deliberately introduce a delay.
To obtain a representative value for the shift in corner frequency, we turn to our observations. Figure 7 shows observed temperature induced variations of a natural frequency of the bridge around 4 Hz. As the temperature changes by more than 20°C, the natural frequency varies by ca. 0.2 Hz. If the difference on our signals were purely due to a change in instrument response corner frequency, we therefore do not expect it to be a difference larger than ∼0.2 Hz. We used this value as a benchmark for simulating the impact of an equal size corner frequency shift in our mathematical test.
The comparison of the original-response and shifted-response signal yielded an apparent relative velocity variation of $0.048\% \frac{\Delta v}{v}$ which is approximately 50 times smaller than the measured variations for the same period. We can therefore exclude that changing instrument responses severely contaminate our measurements.

B. Comparison with prior studies

In order to further check the validity of our evaluation, we draw a comparison to the findings of prior studies. Unfortunately, some of them refer to maximal values of relative velocity variations, observed for certain temperature ranges, while others determined velocity variation rates per °C. Adjusting the units and scales to a uniform level would be convenient for comparison. However, since the investigated media certainly had different material properties, different temperature ranges were examined in each study, and because temperature gradients (size of structure) are not negligible, we leave the values as they were published. To enable a comparison anyway, table II summarizes the range of values we observed.
It is important to note that the studies mentioned below were testing on small-scale bodies compared to our experiment. Additionally, laboratory conditions with well-known sources and experimental setups can be assumed. The active vibration sources they were using are in the kHz-range, therefore multiple scattering plays a role in their analysis, while for the long periods we investigated, scattering can be neglected.
As a first rough estimation the **(author?)** [24] provided comparative values for correcting the temperature influence on ultrasonic velocity in concrete for different temperature steps. They expect corrections of relative velocities ranging from -1.5% to 5% for -4°C to 60°C and dry concrete whereas for water saturated concrete the values differ.
In **(author?)** [6] and reviewed in **(author?)** [5], comparatively high VVRs of $\frac{0.15\%}{^\circ C}$, respectively $\frac{0.16\%}{^\circ C}$ were proposed. These are at the upper limit of the rates we determined. They tested an indoor concrete slab (12 x 5.5 x 0.2 m) over a time interval of one day.
While the outside temperature range was from 17°C to 32°C, the concrete temperature only changed from 26°C to 30°C in the same period. Furthermore, local variations in concrete temperature caused by unilateral heating (sun on outside wall) were observed. Effectively, they determined a linear variation rate for a short period of one day and therefore a small temperature interval of 4°C.
The limits of this temperature interval are beyond the ranges of our experiment, which makes it even harder to compare the two results. Additionally, for our experiment we can assume a more uniform temperature distribution in the medium, although different materials were involved (asphalt covering, concrete, etc.) which behave differently to effects of e.g. insulation and moisture. Especially the blacktop of the road exhibits temperature dependent properties. While for temperatures ≥0°C it is flexible, below freezing temperatures it contributes considerably to the stiffness of the structure[25]. It therefore affects physical properties associated with wave velocity, potentially causing non-linearities in the VVRs.
This behavior, among other factors, can partly account for the variable VVRs we observed (section V) and makes clear why different structures need to be treated separately. The size of the sampled medium, temperature gradients and internal stress states are other factors that can affect a structure's response to temperature fluctuations.

(author?) [7] observed a drop in ultrasonic pulse velocity of 2–3% for an increase in temperature from 0°C to 50°C. This results in a smaller VVR ($\approx \frac{0.06\%}{^\circ C}$) compared to **(author?)** [6] if a linear behavior is assumed. The obtained value is more similar to our average velocity variation rate.
The authors investigated C30/37 (= concrete composition) concrete prisms of 10 x 10 x 30 cm size with a center frequency of 55 kHz. By concentrating on the coda of the signal the whole blocks were sampled, due to multiple scattering in the medium. They had to deal with remnant changes after their first heating/cooling cycle which were attributed to

aging effects or moisture issues. Again, this proves how the obtained values depend on environmental conditions even when evaluating the same body.
Determining a specific calibration factor or pattern to subtract the temperature's effect from velocity changes in an arbitrary structure is problematic. We attempted to eliminate the temperature contribution as described in section V, by determining the VVR and using it to scale and subtract temperature data. This is a first step towards the removal of temperature effects, which can improve the discrimination between harmless temperature- and damage-induced deviations. Furthermore, we might be able to recognize gradual changes in the observed velocity variation rates (VVRs), which could be associated with long-term settling or degradation by ASR (Alkali-Silica Reaction). Future studies, with more accurate temperature measurements and long-term instrument installations ($\geq 1yr$) at their disposal, would be needed to improve the compensation of environmental effects.

C. Temperature effect

A matter to be clarified is, by which process the temperature actually affects the wave velocity in the medium. Figure 8 compares the temperature diffusion into the concrete on a sunny day with fast temperature changes of more than 15 degrees with that on a cloudy day with almost no diurnal temperature cycle. The plots both show temperature series of sensors buried 5 cm (red) resp. 30 cm (blue) deep within the concrete of the bridge. We observe a notable damping and constant temporal shift for the deeper measurements, controlled by the thermal diffusivity of the material. The maxima of the -30 cm daily cycles are delayed by ca. 6 hours with respect to the -5 cm cycles.

Our observed velocity variations correlate much better with -5 cm temperature series in terms of time shift and shape and we obtained qualitatively better results for periods with distinct day-night cycles (February–March). Therefore, we assume that velocity variations are rather induced by temperature gradients between surface and interior than by the change of core temperature represented by the -30 cm measurements.

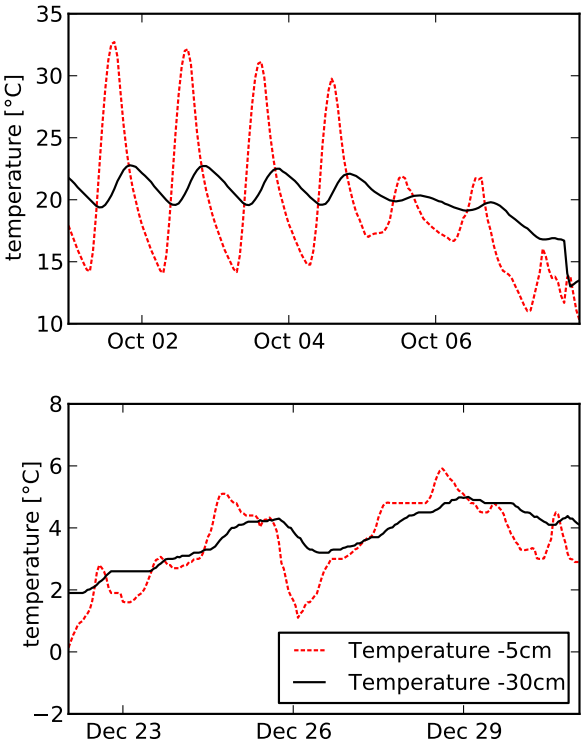

FIG. 8. Temperature measurements at different depths inside the concrete of the deck slab, compared for sunny (top) and cloudy weather (bottom). The temperature in 30 cm depth has a lag of several hours compared to the shallow measurement. On cloudy days, the diurnal variation 5 cm below the surface is minimal, while at sunny days it easily reaches 15°C and more, which leads to strong temperature gradients in the deck slab.

VII. CONCLUSIONS

Due to increased safety norms and aging structures the interest in performing structural health monitoring (SHM) is steadily growing. Different approaches for SHM were proposed in the last decades to replace the well-established but sometimes unreliable visual inspection. Important features for future systems are improved temporal resolution, higher accuracy and lower logistical effort. Consequently, passive monitoring techniques are predestined to fulfill these requirements.
Damage is often indicated by deviations of wave velocity in the medium caused by opening cracks or other disturbed scatterer distribution. Our aim was to extract relative velocity variations using a technique similar to the Passive Image Interferometry[11],

but applied to a small-scale environment. While PII is based on comparison of Green's functions and requires stable and uniform distribution of noise sources, we dealt with uniaxial noise sources in our experimental setup and therefore did not measure GFs. Instead, we showed that it is possible to obtain stable cross-correlation functions for receiver pairs. These are sufficiently sensitive to changes in medium properties (cf.[26]) and can replace GFs in our application.

As a case study, 27 geophones were installed on a highway bridge. These geophones were left to continuously record background noise – mostly generated by traffic – for a duration of approximately 2 months. High traffic activity produced highly stable and reproducible CCFs in which most of the bridges natural frequencies were excited between 2–8 Hz. By comparing hourly CCFs with an all-time average reference stack (of hourly CCFs) via the stretching method, we could show that temperature induced velocity variations can be traced. The velocity variations $\frac{\Delta v}{v}$ cover the ranges depicted in table II, corresponding to temperatures ranging from -23°C to +14°C. In a comparison with previous studies we ascertained that our observed values are in the same order of magnitude.

max. velocity variation rate	$0.14\frac{\%}{^\circ C}$
min. velocity variation rate	$0.024\frac{\%}{^\circ C}$
ave. velocity variation rate	$0.064\frac{\%}{^\circ C}$
rel. velocity variation	-1.5% to +2.1%
temperature range	+14° to -23°C

TABLE II. Results in the 2–8 Hz frequency band. Every velocity variation is presented as a relative deviation from the reference RCF which consists of an average of all CCFs over the whole measurement period. The variation rates were calculated for 24h-intervals, each.

Comparing the two resulting time series (temperature & velocity variation, fig. 5) over the time intervals yielded a strong resemblance. The temporal delay of a few hours between the corresponding values of temperature and velocity variation is associated with thermal diffusion, while velocity variations themselves seem to be linked to temperature gradients.

Due to the strong conformity of the two completely uncorrelated measurements, we proceeded with an estimation a scaling factor between temperatures and wave velocity changes, a velocity variation rate (VVR) per °C. In a linear regression approach to adjust temperature values to velocity variations for each 24h-interval consecutively, we calculated the best fitting VVRs. Although we observed temperature dependent variation rates (average: $\frac{0.064\%}{^\circ C}$), the subtraction of the measured velocity variation and adjusted temperature series in 24h-intervals yielded an almost flat and theoretically temperature independent velocity variation residual. That confirmed the validity of the calculated VVR, and represented a first approach to reduce an environmental effect to thereby accentuate damage induced variations on the structure. Considering very long-term measurements even a gradual change in VVR could indicate structural changes due to damage or aging.

Our method features some advantages concerning monitoring issues. These are high temporal resolution ($\leq$ 1 hour) and continuous applicability with minimal logistical effort and at relatively low cost. Furthermore, we reached good accuracy in determining relative velocity variations and were able to adequately subtract the temperature effect on seismic velocities in the medium.

However, improvements in temperature elimination could be gained by having access to more suitable and extensive temperature measurements inside the bridge, for example between asphalt layer and concrete slab.

The main drawback associated with low frequencies and late-coda analysis is poor spatial resolution. While we are able to recognize minimal velocity changes at high temporal resolution, it would be difficult to localize their exact origin. However, the passive method proposed in this paper could be imagined as a permanent monitoring and early-warning system. The detection of a velocity change would give rise to a visual inspection including punctual tests via ultrasonic pulse methods or e.g. ground-penetrating radar (GPR). In the future, it would be reasonable to perform further experiments that include real damage scenarios to check the sensitivity of our method to damage induced velocity variations. In the course of such an experiment, a cross-check with other methods (US, modal analysis, etc.) could offer valuable clues and help to develop a continuously working monitoring system for civil structures.

ACKNOWLEDGMENTS

We'd like to thank the Karlsruher Institut für Technologie (KIT) for providing the geophones and other equipment, furthermore the Autobahndirek-

tion Nordbayern for allowing us to perform measurements on the Steinachtal bridge, for their cooperation and for giving access to temperature measurements. Thanks to the engineering company Stähler&Knoppik for providing the building plans. We want to express our gratitude to field workers Namat Amat, Stefan Wenk and Tobias Megies who helped install the instruments and to Christoph Sens-Schönfelder, Ernst Niederleithinger, Roel Snieder and Eric Larose for inspiring discussions. This project was partially funded by the Emmy-Noether Program of the DFG (HA7019/1-1).

REFERENCES

[1] Á. Cunha and E. Caetano, "Experimental modal analysis of civil engineering structures", Sound and Vibration **40**, 12–20 (2006).

[2] F. Magalhães, A. Cunha, and E. Caetano, "Vibration based structural health monitoring of an arch bridge: From automated OMA to damage detection", Mech Syst Signal Pr **28**, 212 – 228 (2012).

[3] C. Rainieri and G. Fabbrocino, "Automated output-only dynamic identification of civil engineering structures", Mech Syst Signal Pr **24**, 678 – 695 (2010).

[4] F. Ubertini, A. L. Materazzi, C. Gentile, and F. Pelliccia, "Automatic identification of modal parameters: application to a reinforced concrete arch bridge", Proc. EACS (2012).

[5] T. Planès and E. Larose, "A review of ultrasonic Coda Wave Interferometry in concrete", Cement and Concrete Research **53**, 248 – 255 (2013).

[6] E. Larose, J. de Rosny, L. Margerin, D. Anache, P. Gouedard, M. Campillo, and B. van Tiggelen, "Observation of multiple scattering of khz vibrations in a concrete structure and application to monitoring weak changes", Phys. Rev. E **73**, 016609–016616 (2006).

[7] E. Niederleithinger and C. Wunderlich, "Influence of small temperature variations on the ultrasonic velocity in concrete", AIP Conference Proceedings **1511**, 390–397 (2013).

[8] A. Grêt, R. Snieder, and J. Scales, "Time-lapse monitoring of rock properties with coda wave interferometry", J. Geophys. Res. Solid Earth **111**, 1978–2012 (2006).

[9] O. Lobkis and R. L. Weaver, "On the emergence of the Green's function in the correlations of a diffuse field", J. Acoust. Soc. Am. **110**, 3011–3017 (2001).

[10] N. M. Shapiro, M. Campillo, L. Stehly, and M. H. Ritzwoller, "High-resolution surface-wave tomography from ambient seismic noise", Science **307**, 1615–1618 (2005).

[11] C. Sens-Schönfelder and U. Wegler, "Passive image interferometry and seasonal variations of seismic velocities at Merapi volcano, Indonesia", Geophys. Res. Lett. **33**, L21302 (2006).

[12] U. Wegler and C. Sens-Schönfelder, "Fault zone monitoring with Passive Image Interferometry", Geophys. J. Int. **168**, 1029–1033 (2007).

[13] F. Brenguier, N. M. Shapiro, M. Campillo, V. Ferrazzini, Z. Duputel, O. Coutant, and A. Nercessian, "Towards forecasting volcanic eruptions using seismic noise", Nature Geoscience **1**, 126–130 (2008).

[14] R. Snieder, A. Grêt, H. Douma, and J. Scales, "Coda wave interferometry for estimating nonlinear behavior in seismic velocity", Science **295**, 2253–2255 (2002).

[15] G. Poupinet, W. L. Ellsworth, and J. Frechet, "Monitoring velocity variations in the crust using earthquake doublets: An application to the Calaveras Fault, California", J. Geophys. Res. Solid Earth **89**, 5719–5731 (1984).

[16] O. I. Lobkis and R. L. Weaver, "Coda-wave interferometry in finite solids: Recovery of p-to-s conversion rates in an elastodynamic billiard", Phys. Rev. Lett. **90**, 254302–254306 (2003).

[17] N. M. Shapiro and M. Campillo, "Emergence of broadband Rayleigh waves from correlations of the ambient seismic noise", Geophys. Res. Lett. **31**, L07614 (2004).

[18] C. Hadziioannou, E. Larose, A. Baig, P. Roux, and M. Campillo, "Improving temporal resolution in ambient noise monitoring of seismic wave speed", J. Geophys. Res. Solid Earth **116**, 1978–2012 (2011).

[19] M. Beyreuther, R. Barsch, L. Krischer, T. Megies, Y. Behr, and J. Wassermann, "Obspy: A python toolbox for seismology", Seis. Res. Lett. **81**, 530–533 (2010).

[20] P. F. Dubois, K. Hinsen, and J. Hugunin, "Numerical python", Computers in Physics **10** (1996).

[21] D. Ascher, P. Dubois, K. Hinsen, J. Hugunin, T. Oliphant, *et al.*, "Numerical python", URL: http://www. numpy. org (2001).

[22] P. Cupillard, L. Stehly, and B. Romanowicz, "The one-bit noise correlation: a theory based on the concepts of coherent and incoherent noise", Geophys. J. Int. **184**, 1397–1414 (2011).

[23] T. Keller and C. Menn, "Dauerhaftigkeit von Stahlbetontragwerken: Transportmechanismen – Auswirkungen von Rissen", Technical Report (1992).

[24] British-Standard-Institution, *BS 1881, Part 203, Recommendations for Measurement of Velocity of Ultrasonic Pulses in Concrete*, London (1986).

[25] B. Peeters and G. De Roeck, "One-year monitoring of the Z24-Bridge: environmental effects versus damage events", Earthquake Engineering & Structural Dynamics **30**, 149–171 (2001).

[26] C. Hadziioannou, E. Larose, O. Coutant, P. Roux, and M. Campillo, "Stability of monitoring weak changes in multiply scattering media with ambient noise correlation: Laboratory experiments", J. Acoust. Soc. Am. **125**, 3688–3695 (2009).